Biometals
DOI 10.1007/s10534-010-9384-3

Vesicular distribution of Secretory Pathway Ca^{2+}-ATPase isoform 1 and a role in manganese detoxification in liver-derived polarized cells

Sharon Leitch · Mingye Feng · Sabina Muend · Lelita T. Braiterman · Ann L. Hubbard · Rajini Rao

Received: 16 July 2010 / Accepted: 13 October 2010

Abstract Manganese is a trace element that is an essential co-factor in many enzymes critical to diverse biological pathways. However, excess Mn^{2+} leads to neurotoxicity, with psychiatric and motor dysfunction resembling parkinsonism. The liver is the main organ for Mn^{2+} detoxification by excretion into bile. Although many pathways of cellular Mn^{2+} uptake have been established, efflux mechanisms remain essentially undefined. In this study, we evaluated a potential role in Mn^{2+} detoxification by the Secretory Pathway Ca^{2+}, Mn^{2+}-ATPase in rat liver and a liver-derived cell model WIF-B that polarizes to distinct bile canalicular and sinusoidal domains in culture. Of two known isoforms, only secretory pathway Ca^{2+}-ATPase isoform 1 (SPCA1) was expressed in liver and WIF-B cells. As previously observed in non-polarized cells, SPCA1 showed overlapping distribution with TGN38, consistent with Golgi/TGN localization. However, a prominent novel localization of SPCA1 to an endosomal population close to, but not on the basolateral membrane was also observed. This was confirmed by fractionation of rat liver homogenates which revealed dual distribution of SPCA1 to the Golgi/TGN and a fraction that included the early endosomal marker, EEA1. We suggest that this novel pool of endosomes may serve to sequester Mn^{2+} as it enters from the sinusoidal/basolateral domains. Isoform-specific partial knockdown of SPCA1 delayed cell growth and formation of canalicular domain by about 30% and diminished viability upon exposure to Mn^{2+}. Conversely, overexpression of SPCA1 in HEK 293T cells conferred tolerance to Mn^{2+} toxicity. Taken together, our findings suggest a role for SPCA1 in Mn^{2+} detoxification in liver.

Keywords Manganese · Ca^{2+}-ATPase · Liver · Fractionation · Trans-Golgi network · SPCA1 · ATP2C1

Sharon Leitch and Mingye Feng have contributed equally to this work.

Electronic Supplementary Material The online version of this article (doi:10.1007/s10534-010-9384-3) contains supplementary material, which is available to authorized users.

S. Leitch · M. Feng · S. Muend · R. Rao (✉)
Department of Physiology, Johns Hopkins University School of Medicine, 725 N. Wolfe Street, Baltimore, MD 21205, USA
e-mail: rrao@jhmi.edu

L. T. Braiterman · A. L. Hubbard
Cell Biology, Johns Hopkins University School of Medicine, Baltimore, MD, USA

Introduction

Manganese is among the top five transition elements found in, and extracted from the earth's crust. In biological systems, manganese is an essential trace element required as enzyme cofactor in diverse

Published online: 28 October 2010

cellular pathways, such as the detoxification of harmful superoxide radicals by mitochondrial superoxide dismutase (MnSOD (Weisiger and Fridovich 1973), the urea cycle by arginase (Kanyo et al. 1996), astrocyte glutamine synthetase (Wedler and Ley 1994), and the glycosylation of secretory proteins in the Golgi apparatus by luminal endoglycosidases (Durr et al. 1998). In the clinic, the paramagnetic properties of manganese make it useful as a contrast agent for functional magnetic resonance imaging, following uptake of the ion into cells (Silva and Bock 2008). However, like other trace elements of biological importance, including copper and iron, manganese works as a double-edged sword. Excess manganese confers toxicity by competing with Mg^{2+} binding sites on enzymes such as DNA polymerases where it can make replication error-prone, or by causing metal induced stress and subsequent apoptosis (Beckman et al. 1985). Toxic exposure to manganese results in a central nervous system disorder resembling parkinsonism, more specifically known as manganism (Lucchini et al. 2009), seen in people with occupational exposure to the metal (welders and miners), excess supplementation in total parenteral nutrition, chronic liver disease and illicit drug abuse (Barceloux 1999; Kaiser 2003; McMillan 2005; Lucchini et al. 2009). In the brain, Mn^{2+} deposits in the basal ganglia and globus pallidus, and although the basis for this selective specificity is not clear, the deposition appears to be facilitated by the dopamine transporter, DAT1 (Anderson et al. 2007).

Manganese enters the circulation by intestinal absorption and is conveyed by the portal vein to the liver where it may be returned to the gut via bile (Barceloux 1999). The specific molecular pathways for manganese entry, retention and exit from cells remain to be elucidated. Low affinity Mn^{2+} uptake is likely to be via calcium channels, such as TRPV 5 and 6 located apically on intestinal epithelial cells, store operated channels such as Orai1 or voltage regulated Ca^{2+} channels. The divalent metal transporter, DMT1, has been implicated in active H^{+}-coupled transport of Mn^{2+} into cells (Au et al. 2008, 2009). Members of the metal/bicarbonate symporter family, SLC39a, including ZIP8 and ZIP14, also have divalent metal specificity that includes Mn^{2+}, in addition to Zn^{2+} and Cd^{2+}, and have broad tissue distribution (Girijashanker 2008). Other influx pathways include Mn^{3+}-bound transferrin, which is endocytosed by transferrin receptor-dependent and independent pathways. On the other hand, efflux of ^{54}Mn from hepatocarcinoma derived HepG2 cells was shown to be energy dependent and required intact microtubules, although the transporter responsible for this efflux was not identified (Finley 1998). Recently, it has been proposed that ferroportin, a transporter critical for cellular iron efflux, may also participate in Mn^{2+} clearance (Yin et al. 2010). It was shown that overexpression of ferroportin in HEK 293 cells decreased intracellular Mn^{2+} levels and Mn^{2+} associated toxicity. Thus, while several mechanisms of cellular Mn^{2+} entry have been identified, not much is known about the molecular pathways for Mn^{2+} efflux, particularly into bile.

In this study, we evaluated the expression, localization and role of *S*ecretory *P*athway *C*a^{2+}, Mn^{2+}-*A*TPases (SPCA) in the liver and hepatocyte-derived WIF-B cell line. As members of the superfamily of P-type cation pumps, the Golgi localized SPCA are in a phylogenetically distinct subgroup from the related Ca^{2+}-ATPases of the sarco/endoplasmic reticulum (SERCA) and the plasma membrane Ca^{2+}-ATPases (PMCA). A unique property of SPCA, not shared by SERCA and PMCA pumps, is the ability to transport Mn^{2+} ions with high apparent affinity. Thus, the K_M for ion-dependent ATPase activity of the purified yeast ortholog, Pmr1, was estimated at 20 nM for Mn^{2+}, which is significantly lower than the apparent K_M of 70 nM for Ca^{2+}. Both ions could elicit formation of the catalytic phosphoenzyme intermediate (Mandal et al. 2000). Additionally, Mn^{2+} competitively inhibited Ca^{2+} transport and mutations in the ion binding site abolished transport of both ions, consistent with a common transport mechanism. Similarly, SPCA pumps from *C. elegans* and mammals were shown to transport both Ca^{2+} and Mn^{2+} ions with high affinity (Van Baelen et al. 2001).

Functional evidence for a role of the SPCA pumps in Mn^{2+} homeostasis has largely come from phenotypes of yeast mutants lacking the single SPCA ortholog Pmr1. In standard growth medium, cytosolic Mn^{2+} accumulates in *pmr1* mutants to levels sufficient to scavenge free radicals and bypass defects in cytosolic superoxide dismutase (Lapinskas et al. 1995), inhibit endogenous enzymes such as Ty1 reverse transcriptase (Bolton et al. 2002) or increase viral recombinants (Jaag et al. 2010). Concomitant

loss of Mn^{2+} ions from the Golgi compartments results in underglycosylation of secreted proteins (Durr et al. 1998) and resistance to rapamycin, an inhibitor of the TOR complex (Devasahayam et al. 2007). In fission yeast, loss of Pmr1 and the DMT1-related metal transporter Pdt1 resulted in Mn^{2+}-related, aberrant cell morphology (Maeda et al. 2004). Whereas wild type yeast can tolerate high (millimolar) levels of extracellular Mn^{2+}, *pmr1* mutants are acutely hypersensitive to growth toxicity of this ion, accumulating large amounts of cytosolic Mn^{2+} (Lapinskas et al. 1995). Taken together, these phenotypes reveal the importance of yeast SPCA in Mn^{2+} homeostasis.

Although a physiological role of the SPCA pumps in Mn^{2+} detoxification may be inferred in mammals, direct experimental evidence is wholly lacking. While Mn^{2+} transport has been documented in several systems (Van Baelen et al. 2001), there is no evidence of its biological relevance. Therefore, we sought to determine the expression and localization of SPCA isoforms in the liver, and in a hepatocyte-derived polarized cell line WIF-B, where they may be involved in Mn^{2+} efflux and detoxification. Our findings reveal a novel predominantly sub-surface vesicular localization of SPCA1, unique thus far to liver derived cells, and a functional role in protection against cellular Mn^{2+} toxicity in liver cells.

Methods

Cell lines and culture conditions

WIF-B cells were grown as described previously (Braiterman et al. 2008). Cells were plated at a density of 2.4×10^4 in 6-well plates and fed every other day until use. Untreated cells take about 10 days to fully polarize. HEK 293T cells were cultured at 37°C, 5% CO_2 in DMEM (Invitrogen, Carlsbad, CA) supplemented with 10% FBS (Invitrogen, Carlsbad, CA).

Lentivirus production & infection

Viral particles were packaged in HEK 293T cells by cotransfection of plasmids containing the packaging genome, an envelope glycoprotein (VSVG), Δ8.2R, and a pLK0.1 containing the following target sequences for each knockdown:

hSPCA1: TCATCATGTTGGTTGGCTGG
rSPCA1 sh1: TGATCCCTGTACTGACATC
rSPCA1 sh2: TACTGATTGTTGTCACCGT
hSPCA2: GCGAACCTGTGTGGAAGAAAT (Feng et al. 2010)
DsRed: AGTTCCAGTACGGCTCCAA (Duan et al. 2007)

Supernatant containing viral particles was collected after 48 h. Cells in a 6-well plate were infected with lentivirus containing shRNA of SPCA1 (knockdown) or DsRed (control) using 800 µl of virus for WIF-B cells and 200 µl of virus for HEK 293T cells. Each viral infection was diluted to 1,300 µl with media and 8 µg/ml polybrene was added to WIF-B cells. No polybrene was used in the viral infection of HEK 293T cells. After 24 h, 700 µl of fresh media was added to each well. At 48 h, the cells were trypsinized and transferred to a new 6-well dish. Infected WIF-B and HEK 293T cells were selected for with 10 and 4 mg/ml puromycin, respectively. Uninfected cells were used to establish an adequate concentration of puromycin.

Biotin labeling and Western analysis

Total lysates from animal tissues were extracted by using N^+ buffer (60 mM HEPES, pH 7.4, 150 mM NaCl, 3 mM KCl, 5 mM Na_3EDTA, 3 mM EGTA, and 1% Triton X-100). WIF-B cells were incubated with 0.5 mg/ml of biotin in borate buffer (1 mM boric acid, 154 mM NaCl, 7.2 mM KCl, 1.8 mM $CaCl_2$, pH 9.0) at 4°C for 1 h. Cells were rinsed with quench buffer (20 mM Tris, 120 mM NaCl, pH 7.4) to quench the reaction. Cell lysate in lysis buffer (60 mM HEPES, 150 mM NaCl, 3 mM KCl, 5 mM EDTA, 1 mM sodium orthovanadate, 25 mM sodium pyrophosphate, 50 mM NaF, 1% Triton X-100, pH 7.4, supplemented with protease inhibitor) was incubated with avidin-beads at 4°C for 4 h, and Western blot was performed to analyze the results.

Total yeast lysates were prepared using glass bead methods described in (Sorin et al. 1997). Samples were subjected to SDS/PAGE and Western blotting. Proteins were detected on a Western blot with a 1:5,000 dilution of antibodies purchased from BD Biosciences: anti-EEA1, anti-Golgin84, anti-TGN38,

anti-Rab11 and anti-Calnexin; anti-CE9 and anti-DPP4 were prepared as described before (Nyasae et al. 2003); anti-SPCA2 has been described previously (Xiang et al. 2005). Polyclonal antibodies were raised in rabbit against a 14-amino acid peptide of hSPCA1 (VARFQKIPNGENETMI). Peptide specific antibodies were removed by preincubation with serum for use in negative control. Horseradish peroxidase-coupled anti-rabbit or anti-mouse secondary (1:5,000; GE Healthcare) was used in conjunction with ECL reagents (Amersham Biosciences) to visualize protein bands.

Microsome preparation

Cells (in 1 10-cm dish) were washed twice with PBS and collected into 1 ml of PBS with 5 mM EDTA. The cells were then centrifuged at 10,000g for 2 min and resuspended in 2 ml of solution A (10 mM Tris 7.5, 0.5 mM $MgCl_2$) supplemented with PIC. After being kept on ice for 10 min, the cells were homogenized with 30 strokes in a glass Dounce homogenizer, and 2 ml of solution B (10 mM Tris 7.5, 0.5 M Sucrose, 0.3 M KCl, 6 mM BME, 40 μM $CaCl_2$) was added. The lysate was centrifuged at 10,000g for 20 min to pellet nuclei and mitochondria. The supernant was collected, and centrifuged at 100,000g for 60 min. The microsome pellet was resuspended in 100 μl of solution C (10 mM Tris 7.5, 0.25 M Sucrose, 0.15 M KCl, 3 mM BME, 20 μM $CaCl_2$).

Immunofluorescence microscopy

Cells were grown in 6 well plates containing glass coverslips (22 × 22 mm) and probed with modifications from a previously published staining protocol (Kallay et al. 2006). Once properly polarized the WIF-B cells were pre-extracted with a solution of PHEM buffer (60 mM PIPES, 25 mM HEPES, 10 mM EGTA, and 2 mM $MgCl_2$, pH 6.8) containing 0.025% saponin for 2 min. The coverslips were washed twice for 2 min with a solution of PHEM buffer containing 0.025% saponin and 8% sucrose. The cells were fixed with a solution of 4% PFA and 8% sucrose in PBS for 30 min at room temperature. Coverslips were rinsed three times quickly to rehydrate, and then three times for 5 min each with PBS. A solution of 1% BSA and 0.025% saponin in PBS was used to block for 1 h. The coverslips were probed with the following primary monoclonal antibodies in the blocking solution for 1 h: TGN38 and EEA1 (Transduction Laboratories/BD Biosciences, San Jose, CA) at a dilution of 1:500, HA321 (Nyasae et al. 2003) and MRP2 (Abcam, Cambridge, MA) at a dilution of 1:250. The antibody against SPCA1 is polyclonal and was used at a dilution of 1:500. After incubation with primary antibodies, coverslips were washed 3 times for 5 min with 0.2% BSA in PBS. Secondary antibodies used were anti-rabbit Alexa Fluor 488 at a dilution of 1:2000 and anti-mouse Alexa Fluor 568 at a dilution of 1:1000 (Invitrogen, Carlsbad, CA). The coverslips were incubated in DAPI/PBS (5 mg/ml) for 10 s and rinsed with H_2O and subsequently mounted with Dako Cytomation Fluorescent Mounting Medium (Invitrogen, Carlsbad, CA). Cells were imaged on a Zeiss 710NLO Meta confocal microscope.

Liver: Golgi flotation

Rats were starved for 18 h and livers were removed and perfused with 0.9% NaCl. Rat livers were then homogenized in 0.25 M SKTM solution (5.5 ml/g; 50 mM Tris, 25 mM KCl, 5 mM $MgCl_2$, and 0.25 M sucrose (Bergeron et al. 1982)) with protease inhibitor and 1 mM of PMSF by using Teflon Potter homogenizer. Homogenate was filtered through four layers of gauze and adjusted to 1.02 M sucrose by adding 2 M SKTM. Homogenate was distributed to SW28 ultraclear tubes and same volume of gradient from 1.02 to 0.2 M SKTM was poured onto the top of the homogenate. The gradients were centrifuged at 25,000 rpm for 3.5 h. Five fractions were collected: A, top of gradient to just above white band; B, white band; C, between below white band to the top of the load mark; D, load; E, pellet.

Cell viability

Cell viability was monitored using the MTT assay performed according to Sigma's product information guide for the TOX-1 kit (Sigma–Aldrich, St. Louis, MO) and as previously described (Mosmann 1983). Briefly, following treatment a 5 mg/ml MTT stock solution in PBS was filter sterilized and added to a final concentration of 250 μg/ml and incubated for 2 h at 37°C. Cells were subsequently solubilized by

adding a solution (10% Triton X-100, 0.1 N HCl in isopropanol) equivalent to the volume of the culture medium and mixed until all crystals were uniformly dissolved (not to exceed 2 h). The absorbance of 200 µl of the mixture was read in triplicate on a 96-well plate spectrophotometer (Molecular Devices) at 570 and 630 nm (background). In Fig. 5c, knockdown efficiency of SPCA1 was 52%, and viability of cells with SPCA1 knockdown was normalized to SPCA1 protein expression level accordingly. Uninfected cells responded similarly to control knockdown (DsRed) upon Mn^{2+} treatment.

Results

Isoform specific expression of SPCA in liver and WIF-B cells

Two distinct genes, *ATP2C1* and *ATP2C2*, encode the corresponding SPCA1 and SPCA2 isoforms in vertebrates, including mammals. SPCA2 shows tissue-specific and inducible expression, and is known to be abundant in intestinal epithelium (Vanoevelen et al. 2005) and lactating mammary glands (Faddy et al. 2008). In contrast, SPCA1 is ubiquitously expressed (Vanoevelen et al. 2005) and serves an essential housekeeping role (Okunade et al. 2007). We used isoform-specific polyclonal antibodies to investigate SPCA expression levels in rat liver extracts and in the chimeric liver-derived cell line WIF-B, obtained by fusing rat hepatoma cells with human fibroblasts (Shanks et al. 1994). Western analysis showed a band of ~104 kDa corresponding to SPCA1 in both liver tissue and WIF-B extracts, but we were unable to detect SPCA2 expression in either preparation (Fig. 1a, c). Total membrane fractions from yeast strains devoid of endogenous Ca^{2+} pumps and expressing heterologous human SPCA pumps (Ton et al. 2002; Xiang et al. 2005) were used as positive controls. We conclude that SPCA1 is the relevant isoform for evaluating Mn^{2+} homeostasis in liver.

As a hybrid, WIF-B cells may potentially express both the human and rat form of SPCA1. RT–PCR experiments designed to specifically detect individual forms revealed that mRNA levels of rat SPCA1 are significantly more abundant than hSPCA1 mRNA levels (Fig. 1b). As expected from Western analysis, mRNA for neither rat nor human SPCA2 was detectable (see ahead, Fig. 5).

Vesicular distribution of SPCA1 in liver and WIF-B cells

Confluent cultures of WIF-B cells polarize, forming distinct apical domains between adjacent cells that enclose spherical bile canalicular-like (BC) spaces. Domain-specific distribution of plasma membrane proteins, microtubule architecture and integrity of tight junctions make WIF-B cells a suitable model for membrane trafficking in hepatocytes. Indirect immunofluorescence showed overlapping distribution of SPCA1 and TGN38, consistent with colocalization in the *trans*-Golgi network (Fig. 2) and similar to previous observations in non-polarized cell cultures (Ton et al. 2002). In addition, we observed a novel vesicular distribution of SPCA1, with prominent accumulation of puncta preferentially near the basolateral membrane that has not been previously described in any other cell type. Careful examination of co-stained images with HA321, a basolateral localized protein failed to reveal significant co-localization (Fig. 2 and Electronic Supplemental Movie), suggesting that this population of SPCA1 may reside in vesicles just below the basolateral surface. This possibility was supported by results of cell surface biotinylation (Fig. 3). The presence of two lysines in predicted periplasmic loops of SPCA1 should allow for biotin modification and indeed, low but detectable biotinylation of overexpressed SPCA1 was observed in HEK 293 cells (Feng et al. 2010). However, three independent surface biotinylation experiments failed to reveal the presence of endogenous SPCA1 on the plasma membrane of WIF-B cells, whereas CE9, a known basolateral protein, was abundantly labeled with biotin (Fig. 3). Together, these findings suggest that in WIF-B cells, a significant vesicular pool of endogenous SPCA1 lies close to, but not on, the basolateral membrane.

MRP2 is a multidrug resistance protein that is found on the apical membrane in liver cells. An antibody against the C-terminus of the protein shows the localization of the BC domain. Co-staining with the SPCA1 antibody showed no significant co-localization at the apical membrane, although vesicles close to the apical membrane were observed. Further, co-staining with the early endosomal marker,

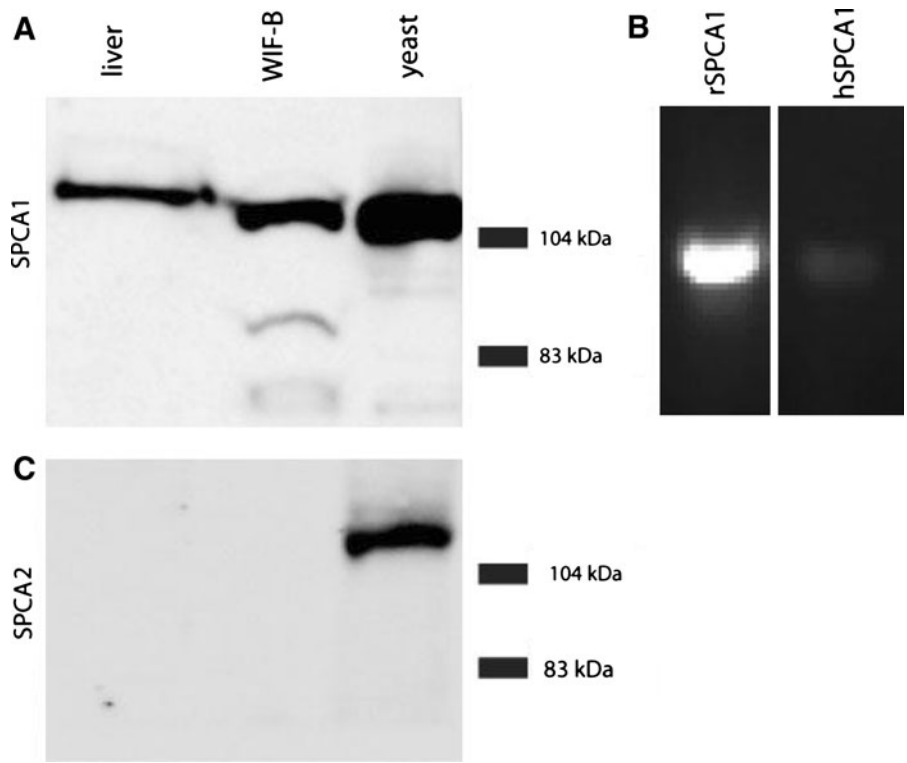

Fig. 1 Isoform specific expression of SPCA pumps in liver and WIF-B cells. **a** and **c**, Western blot using isoform-specific antibody against SPCA1 (*top*) and SPCA2 (*bottom*) of extracts from liver, WIF-B and transgenic yeast strains lacking endogenous calcium pumps that were engineered to express either human SPCA1 or SPCA2, respectively. 100 μg of protein was run in each lane. **b** Reverse-transcription PCR of cDNA from the hybrid WIF-B cell line showing relative transcript levels of rat and human SPCA1

EEA1 showed only low levels of co-localization with SPCA1 in WIF-B cells.

We sought to verify the novel, vesicular distribution of SPCA1 in rat liver by an independent biochemical approach. Liver extracts were fractionated on a discontinuous sucrose gradient and fractions analyzed for membrane marker proteins (Fig. 4A). The Golgi marker protein, Golgin84, was found primarily in fraction b, with smaller amounts in the adjacent lighter (fraction a) and heavier (fraction c) parts of the sucrose gradient. This distribution largely resembled a marker for *trans*-Golgi network membranes, TGN38, also found primarily in fraction b, with significant amounts in fraction a. While SPCA1 was found in fraction b, consistent with Golgi/*trans*-Golgi localization, we also saw substantial levels in fractions c and d, overlapping with fractions containing early endosomal marker, EEA1. In contrast, the distribution of SPCA1 did not overlap significantly with markers for apical or basolateral plasma membranes (DPP4 and CE9), endoplasmic reticulum (calreticulin) or recycling endosomes (Rab11). Figure 4B and Electronic Supplemental Table S1 depicts the yield of membrane markers across the gradient, derived from the individual signal intensity multiplied by the total protein abundance in each fraction. In this analysis, the bulk of TGN38 was found in fraction b whereas the bulk of plasma membrane and ER markers were at the bottom of the density gradients. Due to the low abundance of Golgi membranes, most of SPCA1 was found associated in the fraction also containing early endosome marker EEA1. The identity of this compartment is not likely to be EEA1-containing early endosomes, given the lack of significant co-localization in WIF-B cells, but may be a distinct, basolaterally distributed vesicular population with similar fractionation properties as early endosomes. In summary, we conclude that substantive amounts of the SPCA1 pump are found outside the cisternal stacks of the Golgi/TGN in both polarized WIF-B cells and liver in a unique, hitherto not reported sub-surface membrane pool of vesicles where they may have special functional significance.

Knockdown or overexpression of SPCA1 alters sensitivity to manganese when SPCA2 is absent

It is known that excess Mn^{2+} is detoxified by export into bile by the liver (Papavasiliou et al. 1966), although the identity of the transporter(s) involved in

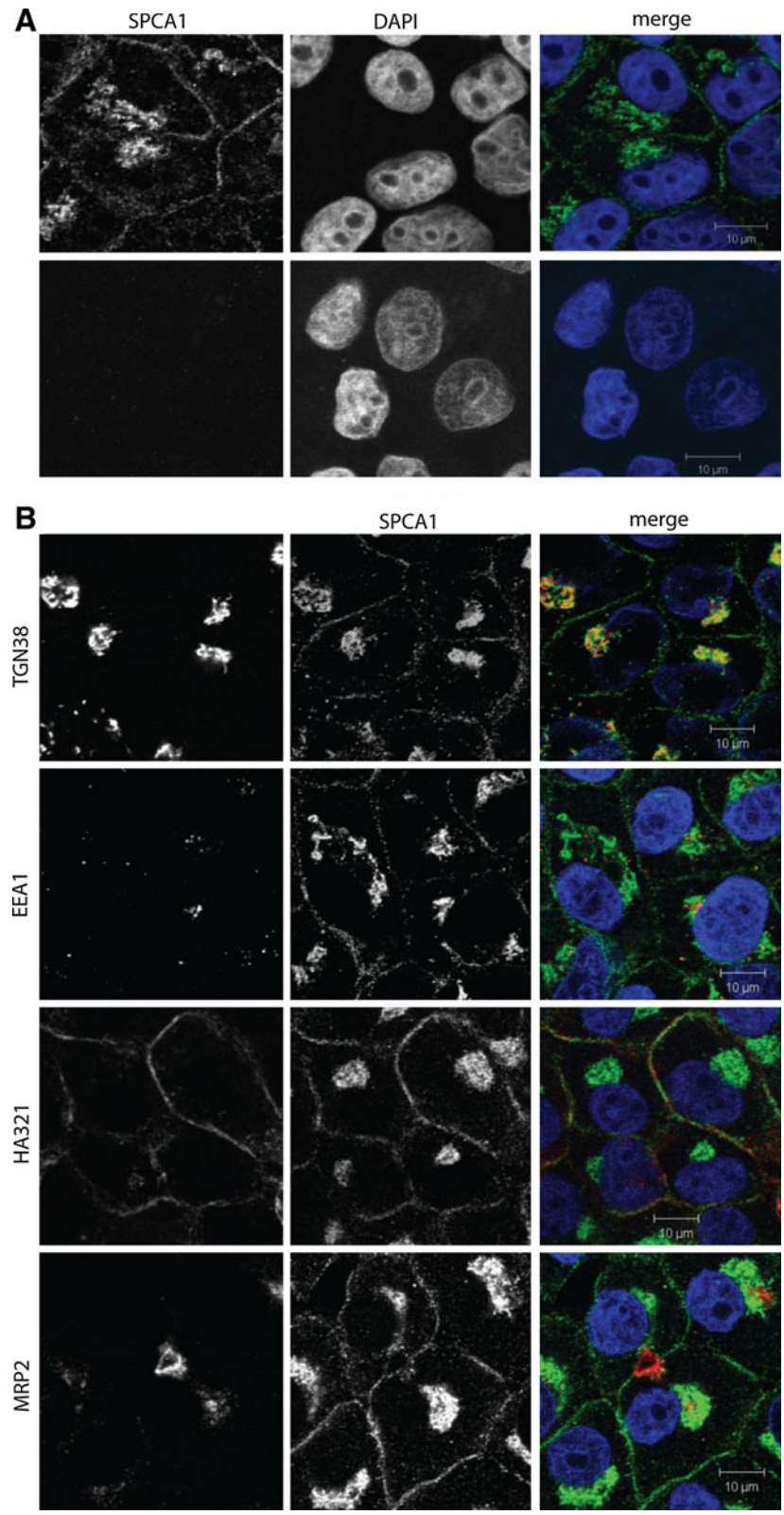

Fig. 2 Dual localization of SPCA1 to Golgi/TGN and sinusoidal/basolateral domain in WIF-B cells. **a** Confocal microscopic images of indirect immunofluorescence from WIF-B cells stained with antibody to SPCA1 in the absence (*top*) or following peptide block (*bottom*), as described in "Methods" section. Nuclei are stained with DAPI. **b**. Confocal microscopic images showing indirect immunofluorescence staining for SPCA1, together with compartmental markers for *trans* Golgi network (TGN38), early endosomes (EEA1), basolateral (HA321) and apical (MRP2) membranes. In the merged images, DAPI stained nuclei (*blue*), SPCA1 (*green*) and individual markers (*red*) are overlaid. (Color figure online)

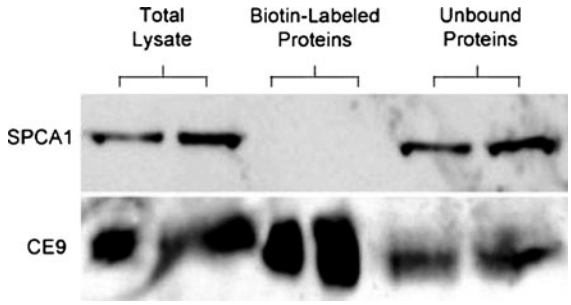

Fig. 3 Surface biotinylation of WIF-B cells fails to detect SPCA1. Western blot following cell surface biotinylation of WIF-B cells, as described in "Methods" section. Protein samples of 60 and 120 μg were obtained from total lysate, biotin labeled proteins (pulled down with avidin beads) and unbound proteins (supernatant remaining after pull down). One of three independent experiments is shown. Note that SPCA1 is not biotinylated, in contrast to the basolateral membrane protein CE9

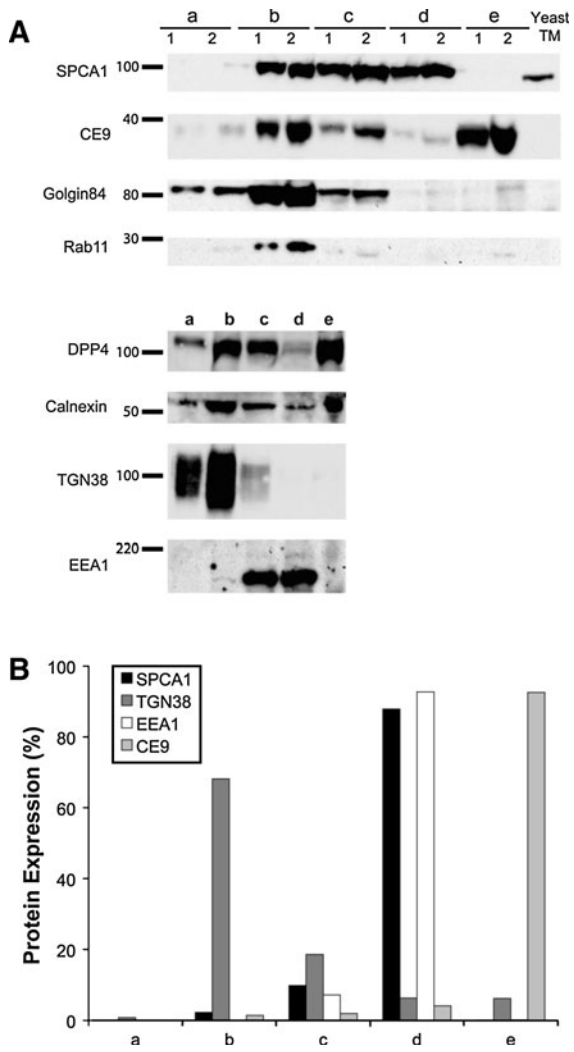

Fig. 4 Sucrose density gradient fractions from rat liver homogenates. **A** Western blots of sucrose gradient fractions from the *top*, fraction *a,* through the bottom, fraction *e,* derived from rat liver homogenates, as described in "Methods" section. Total membranes from yeast expressing hSPCA1 were used as control (Yeast TM). Protein samples were loaded in pairs of 60 μg (*lanes 1*) and 120 μg (*lanes 2*), as indicated, or 60 μg only. **B** Fractional expression of individual proteins was quantified by densitometry and normalized to total protein levels associated with each fraction to show the relative abundance associated with fractions. Expression data (% of total) are tabulated in Electronic Supplemental Table 1. Note the prominent expression of SPCA1 associated with a liver endosomal fraction outside of the Golgi/TGN pool

the efflux mechanism remains to be discovered. To directly assess the functional contribution of SPCA1 in Mn^{2+} detoxification, we engineered a knockdown of rat *ATP2C1* gene expression in WIF-B cells and human *ATP2C1* in HEK 293T cells by infecting with the appropriate shRNA constructs packaged into lentivirus. Partial knockdown of SPCA1 was observed in both WIF-B and HEK 293T cells, by RT–PCR (Fig. 5a and Electronic Supplemental Figure S1B) and Western blotting (Fig. 5b, and Electronic Supplemental Figure S1B). Furthermore, there was no compensatory increase in SPCA2 levels in either cell line. Whereas untransfected or mock-transfected (with DsRed) WIF-B cells polarized 10 days post plating, we observed that partial knockdown of rat SPCA1 slowed cell growth by about 30% and delayed polarization to around day 14 (not shown). No significant change in growth rate was observed with knockdown of SPCA1 in HEK 293T cells, likely because of a significant presence of the SPCA2 isoform in this cell line (Electronic Supplemental Figure S1A). Thus, these preliminary findings suggest that functional expression of SPCA1 is important for growth and polarization of WIF-B cells.

Cells virally infected with control (DsRed) and SPCA1 shRNA were treated with 250 μM $MnCl_2$ for 24 h and assessed for viability by assay of MTT staining. In WIF-B cells with partial knockdown of SPCA1 the inhibitory effect of Mn^{2+} on viability was roughly double (p-value < 0.003) that compared to control (DsRed) cells, whereas uninfected cells resembled DsRed infected cells (not shown). In Fig. 5c, viability is shown relative to growth in the absence of Mn^{2+} in each cell line and normalized for

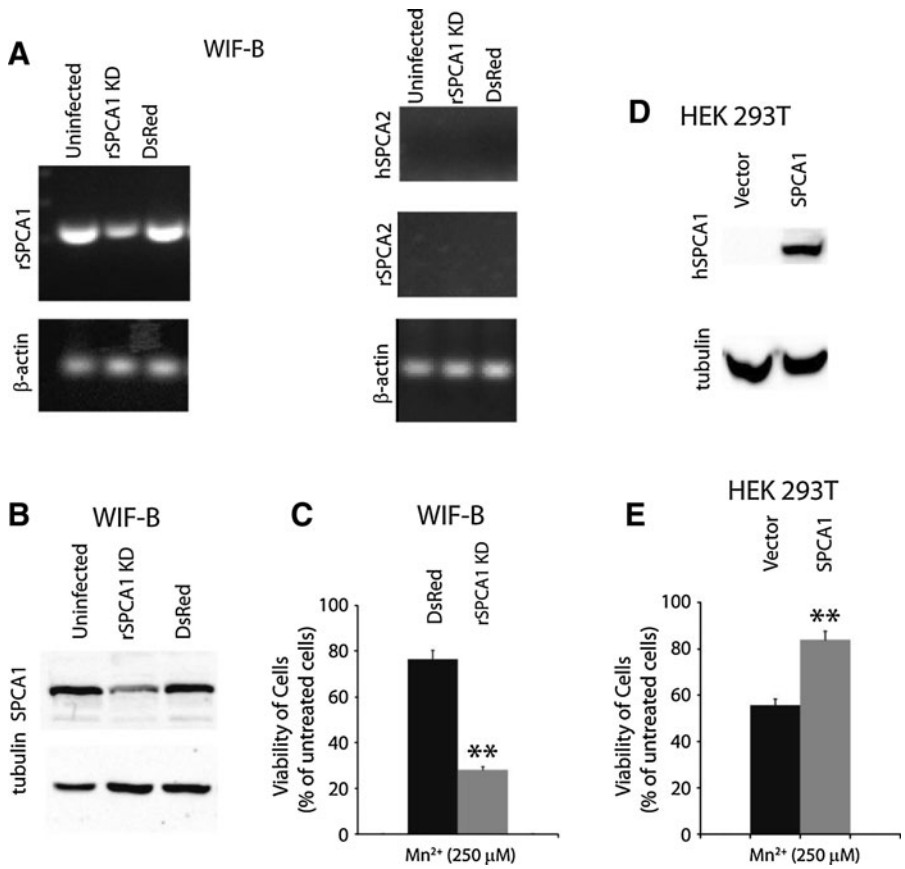

Fig. 5 Mn^{2+} detoxification by SPCA1 in WIF-B and HEK 293T cells. RT–PCR with isoform specific primers (**a**) and Western blot (**b**) showing expression of SPCA1 and SPCA2 in uninfected WIF-B cells, or cells infected with lentivirus targeting knockdown of rSPCA1 or DsRed, as a control. *β*-actin was used as a loading control (**c**). Evaluation of cell viability by MTT assay of WIF-B cells after 24 h exposure to 250 μM $MnCl_2$. In each case, data were normalized to expression level of SPCA1, and viability of cells growing in the absence of $MnCl_2$ was set as 100%, as described in "Methods" section (**d**). Western blot, with anti-HA antibody, showing overpression of HA-tagged SPCA1 in HEK 293T cells (**e**). Viability of HEK 293T cells transfected with empty vector or HA-SPCA1, evaluated by MTT assay following 24 h exposure to 250 μM $MnCl_2$ as described for panel **C**. ** p-value < 0.006

partial knockdown of SPCA1 as described in "Methods" section. As a control for ion specific effects of the knockdown, we also evaluated Cu^{2+} toxicity. There was no difference in the viability of Cu^{2+} treated WIF-B cells with diminished SPCA1 expression in comparison to those with basal SPCA1 levels (Electronic Supplemental Figure S1B). In contrast, in HEK 293T cells, SPCA1 knockdown failed to confer increased susceptibility to either Mn^{2+} or Cu^{2+} toxicity, likely because of redundant expression of the SPCA2 isoform in this cell line (Electronic Supplemental Figure S1C). Conversely, overexpression of SPCA1 in HEK 293T cells conferred significant protection against Mn^{2+} toxicity, relative to vector transfected controls (Fig. 5d, e). Taken together, these observations point to a role for SPCA1 in mediating Mn^{2+} homeostasis and protecting against Mn^{2+} toxicity.

Discussion

The liver is the sole exit route for excess Mn^{2+} via bile excretion into the feces (Papavasiliou et al. 1966). Early experiments in rats showed rapid and saturable biliary clearance, and evidence for active, energy-mediated processes (Klaassen 1974; Ballatori et al. 1987). Studies that followed using the human liver derived cell line, HepG2 (Finley 1998) and hepatocytes derived from skates (Madejczyk et al.

2009), confirmed these observations, although no specific efflux mechanism was identified at a molecular level. The physiological importance of the liver in Mn^{2+} detoxification is best illustrated in patients with cirrhotic livers who have well-documented liver encephalopathy, which is accompanied by excessive serum Mn^{2+} levels and Mn^{2+} deposition in the pallidum, putamen and caudate nucleus of brain (Butterworth 2010). Toxic sequelae of brain Mn^{2+} include neuronal loss and alteration of glutamatergic neurotransmission and cerebral metabolism, leading to cognitive dysfunction, Parkinsonism and ataxia.

Although a multitude of plausible molecular routes for Mn^{2+} uptake have been proposed, transport mechanisms involved in cellular efflux of Mn^{2+} remain largely unexplored. In this study, we make the case for a role of the secretory pathway Ca^{2+}, Mn^{2+}-ATPase, SPCA1, in Mn^{2+} detoxification. First, we show isoform specific expression of *ATP2C1* encoding SPCA1, in rat liver and liver derived hybrid cell line WIF-B. In a mouse model, homozygous knockout of *ATP2C1* was lethal beyond embryonic day 10.5 (Okunade et al. 2007). Consistent with an essential, housekeeping role of this isoform, we found that partial knockdown of *ATP2C1* in WIF-B cells was accompanied by 30% growth inhibition and delay in formation of bile canalicular domains, indicative of a critical role of this pump in polarized hepatocyte growth. A second isoform, SPCA2 encoded by *ATP2C2*, is not expressed in either liver or WIF-B cells, and appears to have a more-specialized, tissue selective function. In HEK 293T cells where there is redundant expression of both isoforms, SPCA1 knockdown did not confer growth inhibitory phenotype, consistent with compensation by SPCA2. We also failed to observe Mn^{2+} dependent changes in expression levels of *ATP2C1* (results not shown), perhaps not surprising given the constitutive and essential function of SPCA1.

Second, the localization of SPCA1 in WIF-B cells is consistent with a role in sequestering Mn^{2+} into the secretory pathway, for exocytic clearance into bile. In addition to the expected Golgi/TGN localization, we observed a novel vesicular population prominent in both liver tissue and liver derived cells. In fully polarized WIF-B cells in culture, SPCA1 localized to endosomes that appeared to be closely associated with the basolateral membrane. We suggest that this pool of endosomes may serve to sequester Mn^{2+} as it enters from the sinusoidal/basolateral domains (Fig. 6). Furthermore, vesicular SPCA1 localized near apical membranes may also serve to accumulate cytosolic Mn^{2+} for delivery into bile. Previous studies have amply demonstrated that SPCA1 can mediate high (nM) affinity, active transport of Mn^{2+}, ensuring accumulation of vesicular Mn^{2+} while cytoplasmic levels remain low (Ton et al. 2002; Vanoevelen et al. 2005). Once packaged within the vesicles, Mn^{2+} may be trafficked as luminal cargo directly to the apical membrane by transcytosis. Alternatively, vesicles may be returned to TGN/recycling compartment where SPCA1 may be sorted away from the luminal cargo. We speculate that there may be specific metal chaperones (proteins or anions such as polyphosphates) that bind and stabilize lumenal Mn^{2+} and improve the efficiency of exocytic clearance into bile. It remains to be determined whether SPCA1 traffics between the vesicular pool and the Golgi/TGN stacks. Although we did not reliably observe Mn^{2+}-dependent changes in SPCA1 localization in WIF-B cells (not shown), there may be constitutive trafficking of the pump between distinct endosomal and Golgi/TGN organellar pools. Given the recent implication of ferroportin in Mn^{2+} efflux in HEK 293 cells (Yin et al. 2010 it would be interesting to determine the localization of this transporter in a polarized liver-derived cell line such as the WIF-B cells. The conspicuous absence of SPCA1 from the bile canalicular membrane leaves open the possibility that additional apical transport mechanisms may facilitate efflux of Mn^{2+} into bile.

We showed that SPCA1 knockdown in WIF-B cells increased Mn^{2+} specific cell death, and conversely, overexpression in HEK 293T cells protected against Mn^{2+} toxicity, consistent with a physiological function of this pump in Mn^{2+} efflux and detoxification. The evaluation of Mn^{2+} mediated cell death may be confounded by opposing effects of cellular Mn^{2+} toxicity and the known anti-oxidant properties of the metal in scavenging free radicals that are likely released during apoptotic or necrotic death (Lapinskas et al. 1995). Thus, we may be underestimating the role of SPCA1 in Mn^{2+} detoxification in WIF-B cells. Adding to this complication is the inviability of complete knockout of SPCA1, demonstrated by embryonic lethality in homozygous mouse knockouts and delayed growth and polarization in cultured cells. Furthermore, the unique architecture of polarized

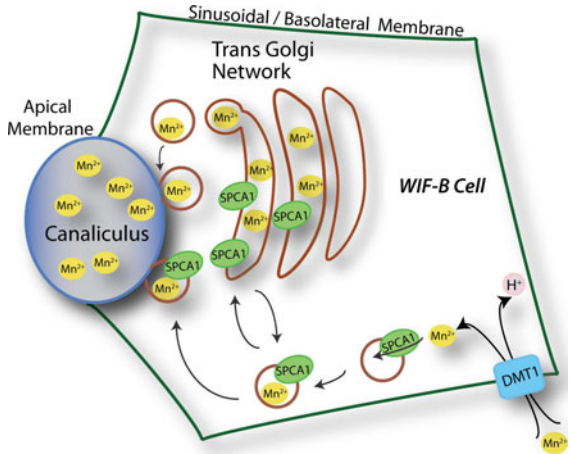

Fig. 6 Cellular model for Mn^{2+} detoxification in the liver cell. At the basolateral or sinusoidal membrane of liver or WIF-B cell, Mn^{2+} is imported by a variety of mechanisms including H^+-coupled symport by the divalent metal transporter DMT1. A basolateral pool of endosomal SPCA1 sequesters Mn^{2+} into the vesicle lumen for transcytotic delivery to the apical membrane and release into bile canaliculus. The model also proposes constitutive trafficking of SPCA1 between vesicular and Golgi/TGN compartments

hepatocytes makes the apical compartment inaccessible in culture and precludes measurement of directed basolateral to apical transport. A more conclusive approach to demonstrate a role of SPCA1 in Mn^{2+} detoxification into bile may require engineering into a mouse model an ion selective mutant of *ATP2C1* that retains Ca^{2+} transport capability, likely to be an essential function, but selectively abrogates Mn^{2+} transport. Mutations selectively defective in Mn^{2+} transport have been identified in the yeast ortholog of the SPCA pumps (Mandal et al. 2000, 2003). If viable, such a Mn^{2+}-selective knockout model may be amenable to more detailed Mn^{2+} clearance studies in vivo.

Acknowledgments This work was supported by a grant from the National Institutes of Health (GM52414) to RR and a predoctoral award from the American Heart Association to MF. We thank Deepti Mohamalawari for excellent technical assistance in preliminary work.

References

Anderson JG, Cooney PT et al (2007) Inhibition of DAT function attenuates manganese accumulation in the globus pallidus. Environ Toxicol Pharmacol 23(2):179–184

Au C, Benedetto A et al (2008) Manganese transport in eukaryotes: the role of DMT1. Neurotoxicology 29(4):569–576

Au C, Benedetto A et al (2009) SMF-1, SMF-2 and SMF-3 DMT1 orthologues regulate and are regulated differentially by manganese levels in *C. elegans*. PLoS One 4(11):e7792

Ballatori N, Miles E et al (1987) Homeostatic control of manganese excretion in the neonatal rat. Am J Physiol 252(5 Pt 2):R842–R847

Barceloux DG (1999) Manganese. J Toxicol Clin Toxicol 37(2):293–307

Beckman RA, Mildvan AS et al (1985) On the fidelity of DNA replication: manganese mutagenesis in vitro. Biochemistry 24(21):5810–5817

Bergeron JJ, Rachubinski RA et al (1982) Galactose transfer to endogenous acceptors within Golgi fractions of rat liver. J Cell Biol 92(1):139–146

Bolton EC, Mildvan AS et al (2002) Inhibition of reverse transcription in vivo by elevated manganese ion concentration. Mol Cell 9(4):879–889

Braiterman LT, Heffernan S et al (2008) JAM-A is both essential and inhibitory to development of hepatic polarity in WIF-B cells. Am J Physiol Gastrointest Liver Physiol 294(2):G576–G588

Butterworth RF (2010) Metal toxicity, liver disease and neurodegeneration. Neurotox Res 18(1):100–105

Devasahayam G, Burke DJ et al (2007) Golgi manganese transport is required for rapamycin signaling in *Saccharomyces cerevisiae*. Genetics 177(1):231–238

Duan X, Chang JH et al (2007) Disrupted-In-Schizophrenia 1 regulates integration of newly generated neurons in the adult brain. Cell 130(6):1146–1158

Durr G, Strayle J et al (1998) The medial-Golgi ion pump Pmr1 supplies the yeast secretory pathway with Ca2+ and Mn2+ required for glycosylation, sorting, and endoplasmic reticulum-associated protein degradation. Mol Biol Cell 9(5):1149–1162

Faddy HM, Smart CE et al (2008) Localization of plasma membrane and secretory calcium pumps in the mammary gland. Biochem Biophys Res Commun 369(3):977–981

Feng M, Grice DM et al (2010) Store-independent activation of Orai1 by SPCA2 in mammary tumors. Cell 143(1):84–98

Finley JW (1998) Manganese uptake and release by cultured human hepato-carcinoma (Hep-G2) cells. Biol Trace Elem Res 64(1–3):101–118

Girijashanker K, He L et al (2008) Slc39a14 gene encodes ZIP14, a metal/bicarbonate symporter: similarities to the ZIP8 transporter. Mol Pharmacol 73(5):1413–1423

Jaag HM, Pogany J et al (2010) A host Ca2+/Mn2+ ion pump is a factor in the emergence of viral RNA recombinants. Cell Host Microbe 7(1):74–81

Kaiser J (2003) Manganese: a high-octane dispute. Science 300(5621):926–928

Kallay LM, McNickle A et al (2006) Scribble associates with two polarity proteins, Lgl2 and Vangl2, via distinct molecular domains. J Cell Biochem 99(2):647–664

Kanyo ZF, Scolnick LR et al (1996) Structure of a unique binuclear manganese cluster in arginase. Nature 383(6600):554–557

Klaassen CD (1974) Biliary excretion of manganese in rats, rabbits, and dogs. Toxicol Appl Pharmacol 29(3):458–468

Lapinskas PJ, Cunningham KW et al (1995) Mutations in PMR1 suppress oxidative damage in yeast cells lacking superoxide dismutase. Mol Cell Biol 15(3):1382–1388

Lucchini RG, Martin CJ et al (2009) From manganism to manganese-induced parkinsonism: a conceptual model based on the evolution of exposure. Neuromolecular Med 11(4):311–321

Madejczyk MS, Boyer JL et al (2009) Hepatic uptake and biliary excretion of manganese in the little skate, *Leucoraja erinacea*. Comp Biochem Physiol C Toxicol Pharmacol 149(4):566–571

Maeda T, Sugiura R et al (2004) Pmr1, a P-type ATPase, and Pdt1, an Nramp homologue, cooperatively regulate cell morphogenesis in fission yeast: the importance of Mn2+ homeostasis. Genes Cells 9(1):71–82

Mandal D, Woolf TB et al (2000) Manganese selectivity of pmr1, the yeast secretory pathway ion pump, is defined by residue gln783 in transmembrane segment 6. Residue Asp778 is essential for cation transport. J Biol Chem 275(31):23933–23938

Mandal D, Rulli SJ et al (2003) Packing interactions between transmembrane helices alter ion selectivity of the yeast Golgi Ca2+/Mn2+-ATPase PMR1. J Biol Chem 278(37): 35292–35298

McMillan G (2005) Is electric arc welding linked to manganism or Parkinson's disease? Toxicol Rev 24(4):237–257

Mosmann T (1983) Rapid colorimetric assay for cellular growth and survival: application to proliferation and cytotoxicity assays. J Immunol Methods 65(1–2):55–63

Nyasae LK, Hubbard AL et al (2003) Transcytotic efflux from early endosomes is dependent on cholesterol and glycosphingolipids in polarized hepatic cells. Mol Biol Cell 14(7):2689–2705

Okunade GW, Miller ML et al (2007) Loss of the Atp2c1 secretory pathway Ca(2+)-ATPase (SPCA1) in mice causes Golgi stress, apoptosis, and midgestational death in homozygous embryos and squamous cell tumors in adult heterozygotes. J Biol Chem 282(36):26517–26527

Papavasiliou PS, Miller ST et al (1966) Role of liver in regulating distribution and excretion of manganese. Am J Physiol 211(1):211–216

Shanks MR, Cassio D et al (1994) An improved polarized rat hepatoma hybrid cell line. Generation and comparison with its hepatoma relatives and hepatocytes in vivo. J Cell Sci 107(Pt 4):813–825

Silva AC, Bock NA (2008) Manganese-enhanced MRI: an exceptional tool in translational neuroimaging. Schizophr Bull 34(4):595–604

Sorin A, Rosas G et al (1997) PMR1, a Ca2+-ATPase in yeast Golgi, has properties distinct from sarco/endoplasmic reticulum and plasma membrane calcium pumps. J Biol Chem 272(15):9895–9901

Ton VK, Mandal D et al (2002) Functional expression in yeast of the human secretory pathway Ca(2+), Mn(2+)-ATPase defective in Hailey–Hailey disease. J Biol Chem 277(8): 6422–6427

Van Baelen K, Vanoevelen J et al (2001) The Golgi PMR1 P-type ATPase of *Caenorhabditis elegans*. Identification of the gene and demonstration of calcium and manganese transport. J Biol Chem 276(14):10683–10691

Vanoevelen J, Dode L et al (2005) The secretory pathway Ca2+/Mn2+-ATPase 2 is a Golgi-localized pump with high affinity for Ca2+ ions. J Biol Chem 280(24):22800–22808

Wedler FC, Ley BW (1994) Kinetic, ESR, and trapping evidence for in vivo binding of Mn(II) to glutamine synthetase in brain cells. Neurochem Res 19(2):139–144

Weisiger RA, Fridovich I (1973) Mitochondrial superoxide simutase. Site of synthesis and intramitochondrial localization. J Biol Chem 248(13):4793–4796

Xiang M, Mohamalawari D et al (2005) A novel isoform of the secretory pathway Ca2+, Mn(2+)-ATPase, hSPCA2, has unusual properties and is expressed in the brain. J Biol Chem 280(12):11608–11614

Yin Z, Jiang H et al (2010) Ferroportin is a manganese-responsive protein that decreases manganese cytotoxicity and accumulation. J Neurochem 112(5):1190–1198